Spectrochimica Acta Part A 79 (2011) 625–630

Contents lists available at ScienceDirect

Spectrochimica Acta Part A: Molecular and Biomolecular Spectroscopy

journal homepage: www.elsevier.com/locate/saa

Quantitative surface enhanced Raman scattering detection based on the "sandwich" structure substrate

Junmeng Zhang[a], Shengchun Qu[a,*], Lisheng Zhang[a,b], Aiwei Tang[a], Zhanguo Wang[a]

[a] Key Laboratory of Semiconductor Materials Science, Institute of Semiconductors, Chinese Academy of Sciences, Beijing 100083, China
[b] Beijing Key Lab of Nano-Photonics and Nano-Structure, Capital Normal University, Beijing 100037, China

ARTICLE INFO

Article history:
Received 16 September 2010
Received in revised form 24 February 2011
Accepted 16 March 2011

Keywords:
SERS
Silver nanoparticles
Silver nanoarrays
AAO template

ABSTRACT

A sandwich structured substrate was designed for quantitative molecular detection using surface enhanced Raman scattering (SERS), in which the probe molecule was sandwiched between silver nanoparticles (SNPs) and silver nanoarrays. The SNPs was prepared using Lee–Meisel method, and the silver nanoarrays was fabricated on porous anodic aluminum oxide (AAO) using electrodepositing method. The SERS studies show that the sandwich structured substrate exhibits good stability and reproducibility, and the detection sensitivity of Rhodamine 6G (R6G) and Melamine can respectively reach up to 10^{-19} M and 10^{-9} M, which is improved greatly as compared to other SERS substrates. The improved SERS sensitivity is closely associated with the stronger electromagnetic field enhancement, which stems from localized surface plasmon (LSP) coupling between the two silver nanostructures. Furthermore, the SERS intensity increased almost linearly as the mother concentration increased, which indicates that such a sandwich structure may be used as a good SERS substrate for quantitative analysis.

1. Introduction

SERS as a powerful analytical tool has gained much attention in biological and chemical field due to its high sensitivity and selectivity [1–5]. Large enhancement of Raman signals on the surfaces of metal nanostructures makes SERS possible to achieve both abundant structural and quantitative information in a nondestructive manner. Additionally, the SERS are often used as a sensitive analytical tool for single molecules detection under optimum conditions. For the detection of single molecules, a very high enhancement (up to 10^{14}–10^{15}) is accordingly required. Theoretically, the strong enhancement is attributed to the so-called hot spots, which may be junctions between nanostructures [6–9].

It is well known that the SERS enhancement strongly depends on the detailed morphology of the nanostructures. The critical issue in achieving the ultimate SERS sensitivity anchors on obtaining the "ideal" substrates, which can yield not only strong SERS effects but also quantitative, reproducible and stable signals. Various methods have been developed to fabricate the "ideal" SERS substrates including the dry methods (such as vacuum deposition, sputtering and lithography) [10–14] and wet methods (such as sol–gel method and electrochemical deposition) [15–18]. The aforementioned methods produce different-shaped nanostructures which are capable of providing the required roughness features for SERS enhancement, such as nanospheres [19], nanowires [20], nanofilms [21], nanoarrays [22,23] and nanorods [24]. In fact, however, these SERS-active substrates mentioned above provide either limited sensitivity or irreproducible Raman signals. Therefore, it is necessary to fabricate an ideal substrate which can construct highly regular and reproducible hot spots.

Up to date, several groups have developed SERS-active sandwich substrates that can exploit LSP coupling between either two nanoparticle layers [25] or one thin film and one nanoparticle layer [26,27], in which the probe molecules are embedded. As reported in previous, the electromagnetic field between two closely spaced SNPs was substantially enhanced by an order of 10^{11} [28]. The SERS intensity of the double sandwich structured substrates based on silver colloid layer is four times stronger than a single substrate [29]. Due to such a strong additional enhancement, the sandwich structured substrates have potential applications in achieving highly improved SERS sensitivity when probe molecules are embedded between the double nanostructures.

In this paper, a sandwich structured substrate was fabricated based on the probe molecules embedded between SNPs and silver nanoarrays, in which SNPs were obtained using Lee–Meisel method [30], and silver nanoarrays were fabricated by electrodepositing silver in the pores of AAO templates. This sandwich structured substrate makes probe molecules surrounded by silver nanostructures in multiple directions, which should help to achieve high SERS sensitivity. The results demonstrate that the detection sensitivity of

* Corresponding author. Tel.: +86 10 82304568; fax: +86 10 82304240.
E-mail address: qsc@semi.ac.cn (S. Qu).

1386-1425/$ – see front matter © 2011 Elsevier B.V. All rights reserved.
doi:10.1016/j.saa.2011.03.045

such a sandwich structured substrate is extremely high, and a good linear relationship between the SERS intensity and the concentrations of probe molecular solutions is obtained.

2. Experimental

2.1. Materials

High purity aluminum (99.999%, 0.25 mm in thickness) was obtained from Beijing Cuibolin Non-Ferrous Technology Developing Co. Ltd. Melamine (99.5%) was purchased from Beijing Chemical Reagents Co, Ltd., and Rhodamine 6G (R6G 95%) was obtained from Sigma–Aldrich Co. Ltd. Other reagents (99.8% silver nitrate, 99.5% boric acid, 99.5% oxalic acid, 85% phosphoric acid, 99.99% chromium trioxide, and 99% trisodium citrate) were purchased from Beijing Chemical works. All chemicals were of analytical grade purity and used as received without further purification.

2.2. Preparation of SNPs

SNPs were prepared according to the Lee–Meisel method. Typically, 45 mg silver nitrate was dissolved in 250 ml deionized water, and the solution was heated to the boiling point. Then 10 ml of a 0.5% trisodium citrate aqueous solution was added into the boiling silver nitrate solution drop by drop, accompanied by vigorous stirring. Afterwards, the mixture was kept boiling for another 10 min and finally it became green-gray. The SNPs prepared in this way was stable for at least several days or weeks.

2.3. Preparation of silver nanoarrays

A highly ordered porous AAO template was fabricated using a classical two-step anodization technique [10,31,32]. Briefly, an aluminum plate (0.25 mm × 50 mm × 75 mm) was anodized in a 0.4 M oxalic acid solution at 8 °C at a constant voltage of 45 V for 1.5 h after annealing and electro-polishing. Then the aluminum oxide film formed by the first anodization was removed and the second anodization was performed for 30 min under the same conditions as the first one. Where after, the anodization voltage was reduced step by step to 12 V to thin the bottom barrier layers at a velocity of 2 V/min.

Silver nanoarrays was deposited in the pores of AAO template by applying AC voltage of 17.8 V with a frequency of 50 Hz for 120 s in the electrolyte containing 0.05 M silver nitrate and 30 g/L boric acid at 8 °C. After electrodeposition, the aluminum substrate on the bottom of AAO template was etched by an aqueous mixture of perchloric acid and copper dichloride, and then the barrier layer was removed in phosphoric acid solution (5 wt%) at ambient temperature. Finally, a transparent-brown thin film was obtained and was kept in absolute ethanol in order to prevent oxidation.

2.4. Measurements

The R6G was used as probe molecule to study the SERS enhancement of the sandwich substrate. R6G was dissolved in deionized water and prepared for various concentrations (2×10^{-8} M to 2×10^{-20} M). Starting with aqueous R6G solution of 2×10^{-8} M, SNPs solution was added to the R6G solutions. 1 ml R6G solution and 1 ml SNPs solution were mixed and, therefore, 2 ml sample with a concentration of 10^{-8} M of R6G molecules was obtained. Solutions of various concentrations from 10^{-8} M to 10^{-20} M, respectively, were prepared using the similar method. The SERS measurements were performed by dropping the R6G/SNPs solution onto the surface of silver nanoarrays, and the schematic illustration of the sandwich structured substrates is given in Fig. 1. The diameter of the spreading area is about 3 mm. After evaporation in drying oven at 70 °C, SERS spectra were recorded using a RENISHAW H13325 Raman spectrophotometer with an excitation laser wavelength of 532 nm and excitation laser power of 5 mW. The laser beam was focused to a spot about 3 μm in diameter by a 50× objective lens. The Raman band of a silicon wafer at 520 cm^{-1} was used to calibrate the spectrometer. In order to see the importance of the presence of silver nanoarrays, SERS spectra of R6G/SNPs solution without silver nanoarrays were also recorded.

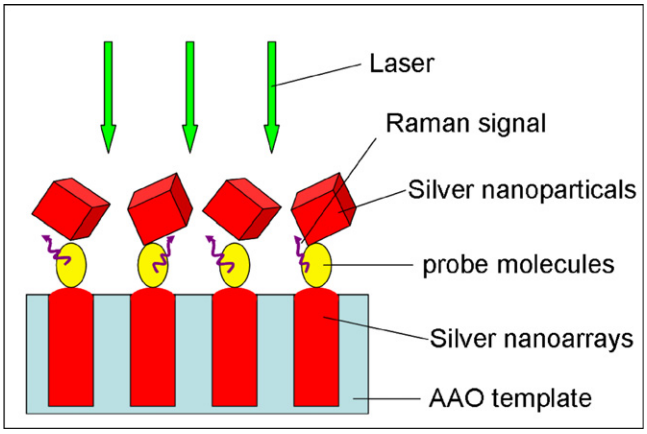

Fig. 1. Schematic diagram of the SNPs/nanoarrays sandwich substrate for SERS.

Another probe molecule, Melamine was diluted to solutions of different concentrations (10^{-3} M to 10^{-9} M) with deionized water. Then they were respectively sandwiched between SNPs and silver nanoarrays for SERS measurements using the same method abovementioned.

The surface morphology of AAO template, silver nanoarrays and sandwich structure was analyzed using a JSM-7401F scanning electron microscope. UV–visible absorption spectra were recorded on a SHIMADZU UV-3101 spectrometer. The resolution was set to 5 nm and the scan region was 300–800 nm.

3. Results and discussion

Fig. 2 displays the UV–visible absorption spectra of SNPs solution and silver nanoarrays. As shown in Fig. 2(a), a single absorption maximum at 436 nm was observed in the UV–visible absorption spectrum of SNPs solution due to the surface plasmon resonance

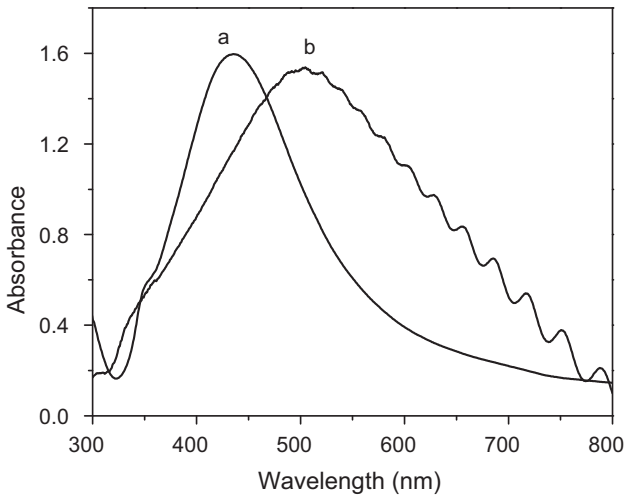

Fig. 2. UV–visible absorption spectra of (a) SNPs solutions and (b) silver nanoarrays fabricated on an AAO template.

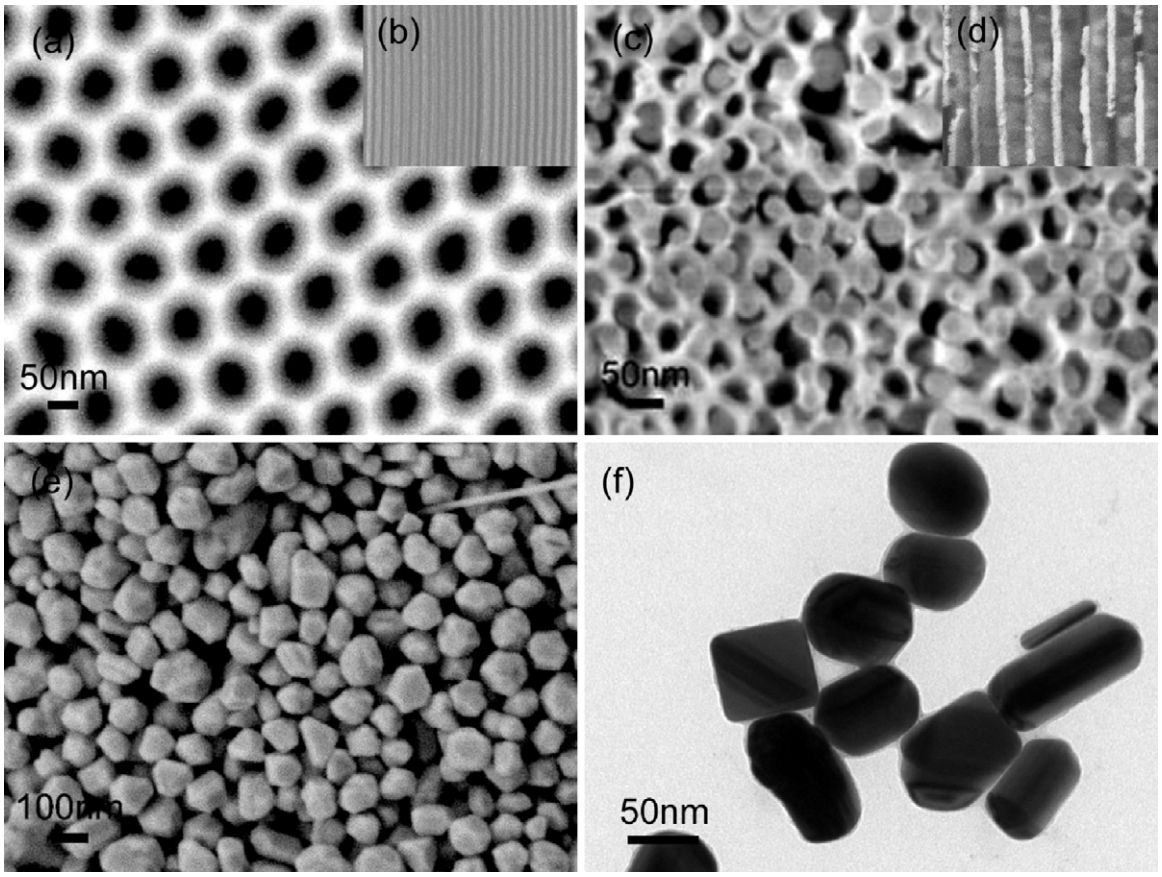

Fig. 3. SEM images of AAO templates (a) in the top view and (b) the cross sectional view, silver nanoarrays (c) in the top view and (d) the cross sectional view, and (e) SNPs adsorbed on silver nanoarrays. (f) TEM image of SNPs.

(SPR) of SNPs. In Fig. 2(b), the characteristic peak of silver nanoarrays deposited on AAO template is located at about 504 nm due to the resonant excitation of plasma oscillations in the confined electron gas of silver nanorods. It should be mentioned that the AAO template is a good transparent matrix for studying the optical properties of silver nanoarrays because the absorption of AAO template is weak at the wavelength region of interest in the present research. The characteristic peak of the spectrum is very close to the 532 nm laser line of Raman spectrophotometer, therefore, the excitation of LSP by the resonant laser line will be very efficient [33,34].

The SEM images of AAO template, silver nanoarrays, and SNPs adsorbed on silver nanoarrays are shown in Fig. 3(a)–(e), respectively. In the top view of AAO template shown in Fig. 3(a), the nanopores of a uniform size are in the form of a perfect two-dimensional array with a hexagonal pattern. The distribution of the pores is very uniform, which indicates that the as-fabricated AAO template is of high quality. In the cross sectional view (Fig. 3(b)), the pores are almost perfectly aligned vertically with respect to the surface of the templates and the height of the AAO templates is estimated to be about 22 μm. Fig. 3(c) and (d) gives the SEM images of silver nanoarrays deposited onto AAO template. It can be observed from the top view (Fig. 3(c)) that the silver nanoarrays is deposited in nearly all the pores of AAO template. They are fixed in the pores with their tips exposed exclusively at the top. As shown in the cross sectional view (Fig. 3(d)), the nanorods is parallel to each other and perpendicular to the Al substrate at the bottom. The average diameter of the nanorods is approximately 50 nm, which corresponds to that of the pores of AAO templates. However, it also can be found that some parts of nanorods in pores are not visible, which may be slipped out from the pores during sampling. The SEM image of the SNPs adsorbed on silver nanoarrays is shown in Fig. 3(e). It can be seen that the distribution of SNPs on the nanoarrays surface is very uniform. Upon dropping the mixed solution onto the silver nanoarrays substrate, the SNPs and probe molecules in the solution will interact and bind to the nanoarrays. Statistically, some of the molecules will be sandwiched in the randomly formed junction between the SNPs and the nanoarrays, where the electromagnetic field would be further enhanced leading to stronger SERS signals. In order to further demonstrate the morphology of the SNPs, the TEM image of SNPs is given in Fig. 3(f). It can be seen that the nanoparticles are irregularly in shape, with many edges on themselves. This property may lead to an increased SERS activity, because the nanoparticles with clear edges can have more enhanced electromagnetic field compared with the nanospheres [35].

For a quantitative analysis, The SERS spectra of the sample solutions with different concentrations of R6G ranging from 10^{-8} to 10^{-20} M were measured. Fig. 4(A) shows the SERS spectra of R6G adsorbed on the sandwich substrates, and the intensity profile of the peak at 1649 cm^{-1} as a function of the concentration of sample solutions is also shown in Fig. 4(B). As shown in Fig. 4(A), it can be seen that the SERS spectrum is very similar to the reported SERS spectrum of R6G. According to previous reports [36], there are three characteristic peaks for identification of R6G molecule: 612 cm^{-1}, 1362 cm^{-1} and 1649 cm^{-1}, in which the 612 cm^{-1} and 1362 cm^{-1} bands are attributed to the characteristic ring in-plane bending mode and the C–C stretching mode, respectively, and the last band is arising from the in-plane mode of ring stretching vibration. For the sake of comparison, we have chosen the strongest band at highest peak at 1649 cm^{-1} as the diagnostic peak, and the integrated intensity of diagnostic bands of each spectrum was used to represent their intensity. It can be seen that the intensity of

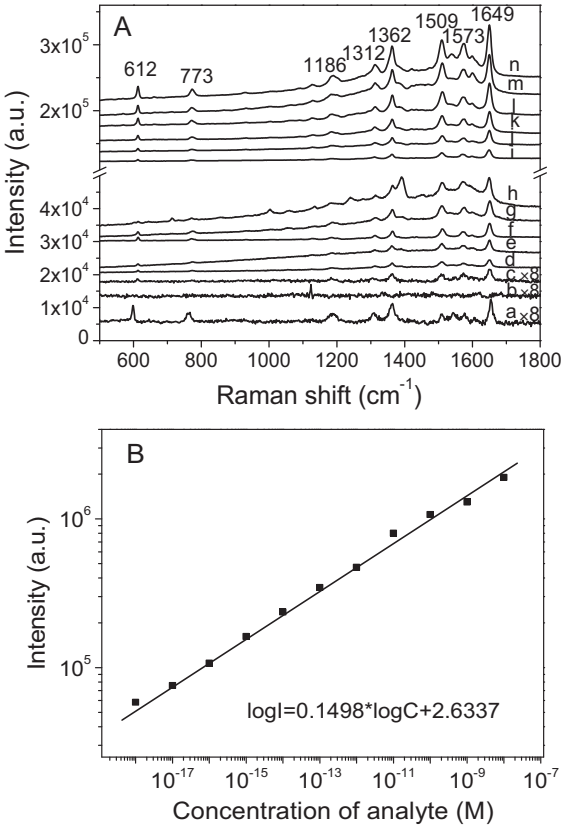

Fig. 4. (A) SERS spectra of R6G embedded in the sandwich structure with the concentrations of (b) 10^{-20} M, (c) 10^{-19} M, (d) 10^{-18} M, (e) 10^{-17} M, (f) 10^{-16} M, (g) 10^{-15} M, (h) 10^{-14} M, (i) 10^{-13} M, (j) 10^{-12} M, (k) 10^{-11} M, (l) 10^{-10} M, (m) 10^{-9} M, (n) 10^{-8} M, and (a) Raman spectrum of 10^{-2} M R6G dropped on a glass slide. (B) The intensity profile of the peak at 1649 cm^{-1} as a function of the concentration of the R6G solutions.

the diagnostic peak of R6G is decreased with the R6G concentration decreasing. As depicted in Fig. 4(B), a good linear relation was observed between the logarithmic concentrations of R6G and the intensities of the diagnostic peak, which provides a calibration for quantitative detection of R6G.

For the SERS spectrum of 10^{-19} M in Fig. 4(A), the characteristic peaks of R6G molecules are distinguishable from the background. Therefore, the 10^{-19} M concentration can be taken as the limit of detection for R6G, which is much lower than that derived from other SERS-active substrates. The SERS enhancement factor (EF) is an important parameter for demonstrating the SERS performance. Herein, we estimate the SERS EF from the standard equation defined as: $EF = I_{SERS}C_{RS}/I_{RS}C_{SERS}$, wherein I_{SERS} and I_{RS} correspond to the Raman intensity of diagnostic band of the probe molecules adsorbed on the SERS substrate and the non-SERS substrate, respectively; C_{SERS} and C_{RS} are, respectively, the concentration of probe molecules under SERS conditions and that under non-SERS conditions, taking into account that the experimental conditions, such as the laser wavelength, laser power, microscope objective lens, and measuring conditions on the substrate, are identical in all cases. As a result, a high Raman EF of 3×10^{16} can be obtained when using C_{SERS} of 10^{-19} M and C_{RS} of 10^{-2} M.

In order to evaluate the SERS contribution from silver nanoarrays in the sandwich substrate, single SNPs as substrate without silver nanoarrays were tested for SERS sensitivity and were compared with the sandwich substrate. The experimental conditions are identical to that for sandwich substrate. Using this single SNPs substrate, the lowest detectable concentration of R6G was around 10^{-16} M (Fig. 5), which was lower than the 10^{-19} M of sandwich substrate. Therefore, the importance of the presence of silver nanoarrays was proved.

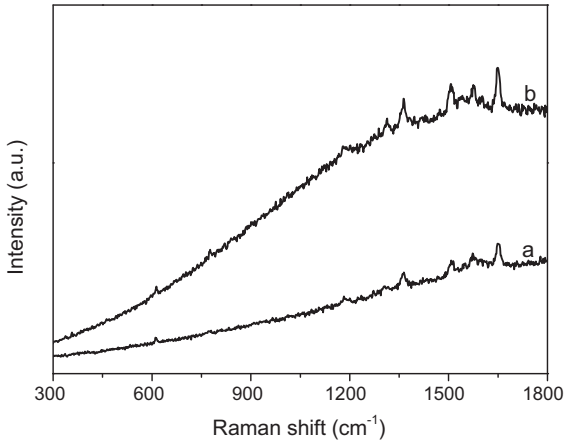

Fig. 5. SERS spectra of R6G in the R6G/SNPs solutions with concentrations of 10^{-16} M and 10^{-15} M, respectively.

As we know, R6G is electronically resonant molecule for SERS due to its electronic energy levels. When the laser line is focused on 532 nm, the contribution to high Raman EF from the electronic resonance of R6G with laser wavelength is also very large. Therefore, to be precise, the Raman signal obtained should be a surface enhanced resonance Raman scattering (SERRS), not pure SERS effect. Then, we chose one non-electronically resonant molecule, Melamine, as another probe molecule to measure SERS performance of the above substrate. Melamine is one of nitrogen-containing organic compounds, which adulterated intentionally in milk products can invite dangers in public-health. Fig. 6(A) indicates the intensity of Melamine's characteristic peaks decreases with decreasing Melamine concentration. Significantly, it is observed that the detection limit of the sandwich substrate for Melamine could reach as low as 10^{-9} M. Moreover, Fig. 6(B) reveals a linear relation between the SERS intensity and Melamine concentration similar to the case for R6G detection.

Based on the above observations, the detection sensitivity of the sandwich substrate is higher than other SERS substrates no matter the probe molecular is resonant or non-resonant. The electromagnetic mechanism is considered to play an important role in the additional Raman enhancement. In recent studies [29,37], a cooperative coupling effect of double SERS-active nanostructures was proposed to account for the additional SERS intensity. It has been suggested that the interaction between LSP of SNPs and LSP of silver nanoarrays are responsible for such enhancement. When SNPs is irradiated with light, the oscillating electrons in the SNPs induce electron oscillations in the silver nanoarrays, thus producing LSP with the frequency equal to that of SNPs. The LSP in SNPs is coupled to the LSP in the silver nanoarrays, resulting in a new set of coupled LSP modes. In our study, the optical response range of silver nanoarrays is close to the laser line, and also overlaps well with the absorption band of SNPs, thus LSP resonance of the sandwich substrate can be easily obtained. As a result, it is possible for the strong SERS enhancement due to the hot spots in the junction between the two silver substrates resulting from the LSP resonance coupling. Statistically, some of the probe molecules can be sandwich in the junctions where the hot spots exist, which makes the SERS signals become stronger. Therefore, it is proposed that the additional Raman enhancement of this substrate is attributed to the existence of strong electromagnetic field generated by the cooperative coupling of LSP of SNPs and LSP of silver nanoarrays in the junctions between the two silver nanostructures.

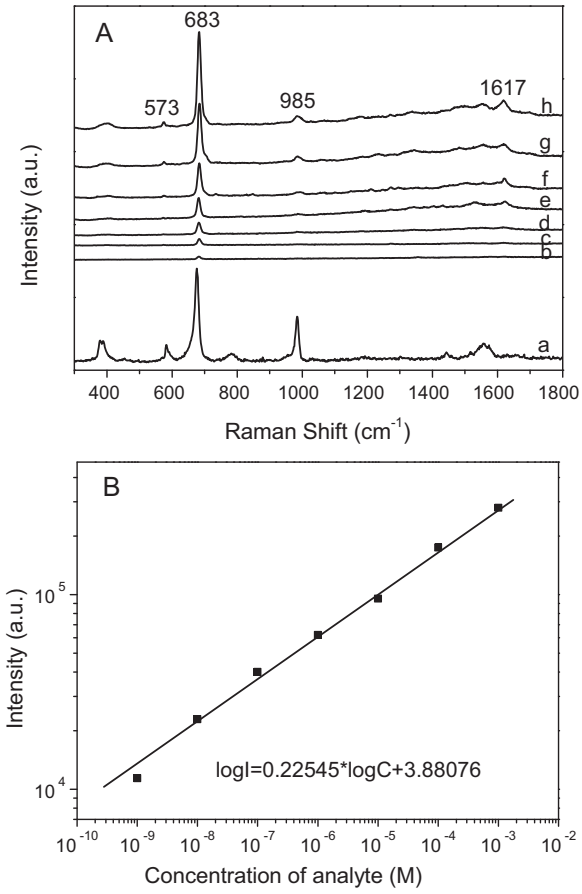

Fig. 6. (A) SERS spectra of Melamine embedded in the sandwich structure with the concentrations of (b) 10^{-9} M, (c) 10^{-8} M, (d) 10^{-7} M, (e) 10^{-6} M, (f) 10^{-5} M, (g) 10^{-4} M, (h) 10^{-3} M, and (a) Raman spectrum of solid Melamine. (B) The intensity profile of the peak at 683 cm^{-1} as a function of the concentration of the Melamine solutions.

Reproducibility is another important parameter in SERS performance. Fig. 7 shows the reproducibility test of SERS spectra of 10^{-12} M R6G obtained from six randomly selected points on the surface of sandwich substrate. It can be observed in the SERS spectra that remarkable reproducibility is achieved in the characteristic peaks of R6G at 612, 1362, and 1649 cm^{-1}. In order to analyze the reproducibility quantitatively, the integrated intensities of each spectrum at 1649 cm^{-1} is calculated, and a 14.1% relative standard deviation is obtained. This indicates that the sandwich-based SERS of our substrate has good reproducibility. The reasons for the good reproducibility of SERS can be summarized as follows: our silver nanoarrays is very uniform in diameter and length and the SNPs are well-distributed on the surface of nanoarrays. Therefore, the number of the junctions irradiated by the focused laser beam is similar in each measurement. On the other hand, the R6G molecules and SNPs are mixed homogeneously before dropping on the surface, which makes the surface concentration of R6G become relatively uniform on the entire surface. It should be mentioned that the SERS activity of the sandwich substrate preserved almost the same after keeping in absolute alcohol for one week. It indicates that this sandwich substrate has good stability, which is important for practical applications in the future.

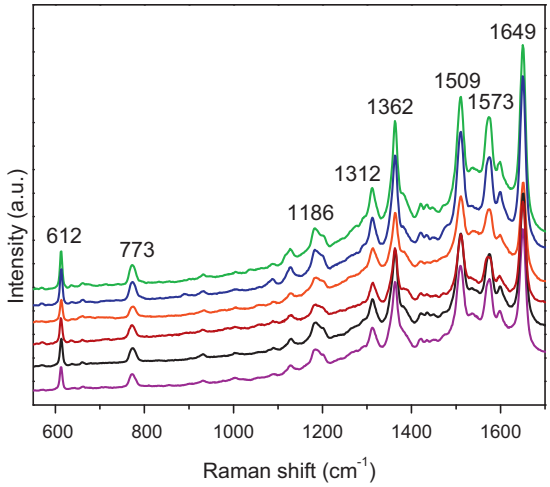

Fig. 7. SERS spectra of 10^{-12} M R6G obtained from six randomly selected points on the surface of sandwich substrate.

4. Conclusions

In conclusion, a simple and reproducible SERS-active sandwich substrate based on probe molecular embedded between SNPs and silver nanoarrays has been presented. This sandwich structured substrate exhibits a good linear relationship between the SERS intensity and the concentration of probe molecular solutions. The detection limit of this substrate can reach extremely low for either resonant or non-resonant probe molecular, which is significantly superior to other SERS-active substrates. This improvement of SERS sensitivity is attributed to the enhanced local electromagnetic field associated with LSP produced by plasmon cooperative coupling between the SNPs and the silver nanoarrays. In addition, the sandwich substrate shows excellent reproducibility and good stability. Therefore, a SERS sensor based on this SNPs/nanoarrays sandwich structured substrate used for rapid, sensitive, and quantitative detection of molecules in chemistry or biology fields will be realized in the coming future.

Acknowledgments

This work was financially supported by the National Basic Research Program of China (973 Program) under Grant No. 2010CB933800 and National Natural Science Foundation of China under Grant Nos. 61076009, 60736034 and 50990064.

References

[1] G.V. Pavan Kumar, B.A. Ashok Reddy, M. Arif, T.K. Kundu, C. Narayana, J. Phys. Chem. B 110 (2006) 16787–16792.
[2] Z.P. Zhou, D.Y. Wan, X.Y. Dou, L. Song, X.Q. Yan, D.F. Liu, H.J. Yuan, Y. Gao, J.X. Wang, L.F. Liu, W.Y. Zhou, S.S. Xie, Physica E 28 (2005) 360–364.
[3] Y.P. Sun, W. Song, X. Zhu, R. Zhang, Q.Y. Pang, Z.R. Zhang, H.F. Yang, J. Raman Spectrosc. 40 (2009) 1306–1311.
[4] D.A. Stuart, C.R. Yonzon, X.Y. Zhang, O. Lyandres, N.C. Shah, M.R. Glucksberg, J.T. Walsh, R.P. Van Duyne, Anal. Chem. 77 (2005) 4013–4019.
[5] C.S. Levin, S.W. Bishnoi, N.K. Grady, N.J. Halas, Anal. Chem. 78 (2006) 3277–3281.
[6] E.C. Le Ru, P.G. Etchegoin, M. Meyer, J. Chem. Phys. 125 (2006) 204701.
[7] J.P. Camden, J.A. Dieringer, Y.M. Wang, D.J. Masiello, L.D. Marks, G.C. Schatz, R.P. Van Duyne, J. Am. Chem. Soc. 130 (2008) 12616–12617.
[8] S.J. Lee, A.R. Morrill, M. Moskovits, J. Am. Chem. Soc. 128 (2006) 2200–2201.
[9] K. Imura, H. Okamoto, M.K. Hossain, M. Kitajima, Nano Lett. 6 (2006) 2173–2176.
[10] L.S. Zhang, Y. Fang, P.X. Zhang, Spectrochim. Acta A 69 (2008) 91–95.
[11] V.L. Schlegel, T.M. Cotton, Anal. Chem. 63 (1991) 241–247.
[12] L.S. Zhang, P.X. Zhang, Y. Fang, Anal. Chim. Acta 591 (2007) 214–218.
[13] L.S. Zhang, Y. Fang, P.X. Zhang, Chem. Phys. Lett. 451 (2008) 102–105.
[14] S. Chattopadhyay, H.C. Lo, C.H. Hsu, L.C. Chen, K.H. Chen, Chem. Mater. 17 (2005) 553–559.
[15] W.H. Ke, D.F. Zhou, J.Z. Wu, K. Ji, Appl. Spectrosc. 59 (2005) 418–423.
[16] C. Schmuck, P. Wich, B. Kustner, W. Kiefer, S. Schlucker, Angew. Chem. Int. Ed. 46 (2007) 4786–4789.
[17] N. Leopold, B. Lendl, J. Phys. Chem. B 107 (2003) 5723–5727.

[18] L. Rivas, S. Sanchez-Cortes, J.V. Garcia-Ramos, G. Morcillo, Langmuir 17 (2001) 574–577.
[19] C.H. Wang, D.C. Sun, X.H. Xia, Nanotechnology 17 (2006) 651–657.
[20] I. Yoon, T. Kang, W. Choi, J. Kim, Y. Yoo, S.W. Joo, Q.H. Park, H. Ihee, B. Kim, J. Am. Chem. Soc. 131 (2009) 758–762.
[21] L.A. Dick, A.D. McFarland, C.L. Haynes, R.P. Van Duyne, J. Phys. Chem. B 106 (2001) 853–860.
[22] Q. Zhou, Y. Yang, J. Ni, Z.C. Li, Z.J. Zhang, Physica E 42 (2010) 1717–1720.
[23] L.S. Zhang, P.X. Zhang, Y. Fang, J. Colloid Interface Sci. 311 (2007) 502–506.
[24] R.L. Zong, J. Zhou, Q. Li, B. Du, B. Li, M. Fu, X.W. Qi, L.T. Li, J. Phys. Chem. B 108 (2004) 16713–16716.
[25] C. Shi, H. Yan, C. Gu, D. Ghosh, L. Seballos, S.W. Chen, J.Z. Zhang, B. Chen, Appl. Phys. Lett. 92 (2008) 103107.
[26] J.K. Daniels, G. Chumanov, J. Phys. Chem. B 109 (2005) 17936–17942.
[27] C.J. Orendorff, A. Gole, T.K. Sau, C.J. Murphy, Anal. Chem. 77 (2005) 3261–3266.
[28] H.X. Xu, J. Aizpurua, M. Kall, P. Apell, Phys. Rev. E 62 (2000) 4318–4324.
[29] C.D. Keating, K.K. Kovaleski, M.J. Natan, J. Phys. Chem. B 102 (1998) 9414–9425.
[30] P.C. Lee, D. Meisel, J. Phys. Chem.-US 86 (1982) 3391–3395.
[31] S.B. Chaney, S. Shanmukh, R.A. Dluhy, Y.P. Zhao, Appl. Phys. Lett. 87 (2005) 031908.
[32] N. Ji, W.D. Ruan, C.X. Wang, Z.C. Lu, B. Zhao, Langmuir 25 (2009) 11869–11873.
[33] G.H. Gu, J. Kim, L. Kim, J.S. Suh, J. Phys. Chem. C 111 (2007) 7906–7909.
[34] G.H. Gu, J.S. Suh, J. Raman Spectrosc. 41 (2010) 624–627.
[35] A. Gutes, C. Carraro, R. Maboudian, ACS Appl. Mater. Interf. 1 (2009) 2551–2555.
[36] X.T. Wang, W.S. Shi, G.W. She, L.X. Mu, S.T. Lee, Appl. Phys. Lett. 96 (2010) 053104.
[37] Y.A. Yang, A.M. Bittner, K. Kern, J. Solid State Electrochem. 11 (2007) 150–154.